VU VRIJE UNIVERSITEIT AMSTERDAM

VU Research Portal

Consequences of foreland basin development on thinned continental lithosphere: Applications to the Aquitane basin (SW France)

Desegaulx, P.; Kooi, H.; Cloetingh, S.A.P.L.

published in
Earth and Planetary Science Letters
1991

document version
Publisher's PDF, also known as Version of record

Link to publication in VU Research Portal

citation for published version (APA)
Desegaulx, P., Kooi, H., & Cloetingh, S. A. P. L. (1991). Consequences of foreland basin development on thinned continental lithosphere: Applications to the Aquitane basin (SW France). *Earth and Planetary Science Letters*, *106*, 116-132.

General rights
Copyright and moral rights for the publications made accessible in the public portal are retained by the authors and/or other copyright owners and it is a condition of accessing publications that users recognise and abide by the legal requirements associated with these rights.

- Users may download and print one copy of any publication from the public portal for the purpose of private study or research.
- You may not further distribute the material or use it for any profit-making activity or commercial gain
- You may freely distribute the URL identifying the publication in the public portal ?

Take down policy
If you believe that this document breaches copyright please contact us providing details, and we will remove access to the work immediately and investigate your claim.

E-mail address:
vuresearchportal.ub@vu.nl

Download date: 14. Sep. 2021

Earth and Planetary Science Letters, 106 (1991) 116–132
Elsevier Science Publishers B.V., Amsterdam

[XLeP]

Consequences of foreland basin development on thinned continental lithosphere: application to the Aquitaine basin (SW France)

Pascal Desegaulx [a], Henk Kooi [b] and Sierd Cloetingh [b]

[a] *Institut Français du Pétrole, 1 et 4 av. du bois Préau, 92506 Rueil Malmaison, France*

[b] *Department of Sedimentary Geology, De Boelelaan 1085, 1081 HV Amsterdam, The Netherlands*

Received December 21, 1990; revised and accepted June 10, 1991

ABSTRACT

We present an analysis of the consequences of foreland basin development on thinned continental lithosphere, inherited from pre-orogenic phases of extension. Bathymetry at the transition from pre-orogenic extensional basin to foreland basin and compaction of pre-orogenic sediments contribute to the accommodation space for foreland basin sediments and thrust loads. In addition, the extension-induced transient thermal state of the lithosphere, results in ongoing thermal subsidence, and a flexural rigidity which changes through time. Quantitative modelling of the phase of extension and the foreland basin stage of the Aquitaine basin (southern France) shows that the inherited transient thermal state of the lithosphere contributes significantly to (1) the total foreland basin depth and width, (2) the post-compressional subsidence history, and (3) the cratonward onlap pattern. Accounting for the thermo-mechanical effects of pre-orogenic extension significantly reduces the estimates of both the flexural rigidity (30–43% for the Aquitaine basin) and the required topographic or thrust load (40% for the Aquitaine basin) at foreland basins. Emplacement of thrust loads below sea level, as expected in a pre-orogenic extensional basin setting, further reduces the required topographic load. This sheds light on the wide range of flexural rigidity values reported for continental lithosphere from foreland basin modelling studies, and explains, in many instances, the inferred 'hidden load' or subsurface load in flexural modelling studies at foreland basins. The present study has shown that pre-orogenic extension phases significantly affect the record of vertical motion and the stratigraphy of the Aquitaine basin and is probably important for foreland basin evolution in general.

1. Introduction

During the last decade considerable progress has been made in understanding the subsidence mechanisms of foreland basins [1, 2, 3]. Numerous studies have revealed that subsidence of foreland basins is mainly controlled by the flexural response of the lithosphere to topographic loading. However, it has also been shown that topographic loading only is not always sufficient to explain the observed deflection and/or gravity data [4, 5, 6]. The required subsurface or 'hidden' load has been attributed to either dense obducted blocks [4, 7, 8] or forces acting on the subducted slab [9, 5, 10]. A feature in foreland basin evolution, which has been largely ignored up to now, with the exceptions of Stockmal et al. [11] and Chery et al. [12], is the generally observed phase of extension preceding the compressional phase of mountain building. In western Europe, many orogenic belts are emplaced nearby or on top of extensional structures. The Betic chain in southern Spain and its prolongation to the northeast (Balearic chain) was emplaced during the Cenozoic in an area subjected to Mesozoic extensional tectonics [13, 14]. North of the Betic zone, the Iberic Cordillera was formed close to an Early Cretaceous aulacogen [15]. The Pyrenees are another clear example of this type of orogenic belt. The Pyrenean chain, at the boundary between the Iberian and European plates, resulted partly from inversion of Late Jurassic to Albian deep basins [16].

In many cases, the insufficient topographic load can be largely due to the fact that a significant part of the overthrusted load has been emplaced on a passive margin [11]. A phase of extension has

0012-821X/91/$03.50 © 1991 – Elsevier Science Publishers B.V. All rights reserved

implications not only for crustal thickness and the distribution of pre-orogenic sediments, but also has a strong bearing on the thermal structure of the lithosphere during and probably even after the orogenic phase. In the following we will first discuss the effects of a pre-orogenic phase of extension on: (1) the accommodation space for sediment during the foreland basin stage; (2) the evolution of flexural rigidity of the lithosphere during the foreland basin stage. Both of these aspects are of importance for the history of foreland basin subsidence and for the stratigraphic record. Subsequently, we will quantify the influence of inherited thermal structure of the lithosphere on the thermo-mechanical evolution of foreland basins, using the Aquitaine basin as an example. To analyse the thermal history and flexural rigidity of the area, we first model the extensional tectonics of the Aquitaine basin using constraints provided, amongst others, by deep seismic data. Finally, we will discuss the model predictions in the light of foreland basin subsidence in general and the subsidence history of the Aquitaine basin in particular.

2. Pre-orogenic extension and foreland basin subsidence

2.1. *Effect of extension on accommodation space for sediments*

Extensional basins, in particular those involved in a subsequent orogeny, are often associated on the seaward side with a deep water slope and rise setting, such as at rifted continental margins (Fig. 1). This water body provides accommodation space, not only for advancing thrust loads, but also for early foreland basin sediments. In this context it is important to realize, based on simple isostatic principles, that bathymetry provides accommodation space for a sediment thickness of at least 2–3 times the available water depth.

A second contribution to the accommodation space for foreland basin sediments is provided by compaction of the sediments deposited during the extensional basin phase upon subsequent burial. Given the observed foreland basin sediment thickness z_{fo}, the foreland basin sediment thickness in the absence of compaction of underlying sediments z_f and the underlying extensional basin

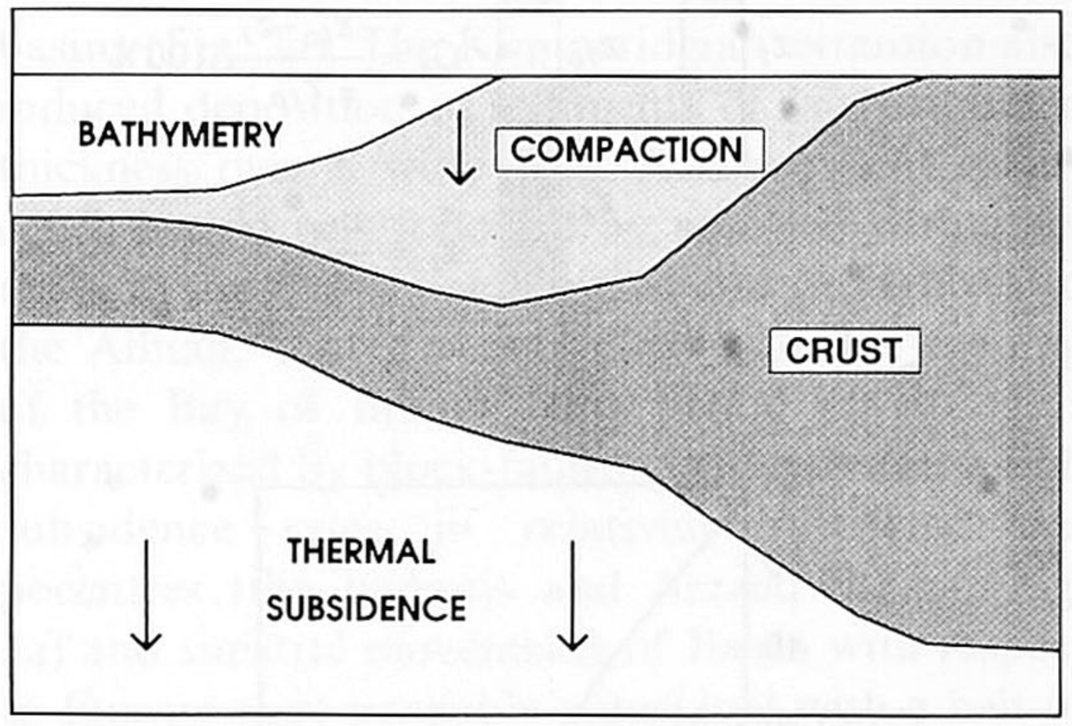

Fig. 1. Schematic illustration of three features associated with pre-orogenic extensional basins, which contribute to the accommodation space for foreland basin sediments and thrust loads: (1) pre-orogenic bathymetry; (2) compaction of pre-orogenic sediments; (3) ongoing thermal subsidence induced by pre-orogenic lithospheric extension.

sediment thickness z_e as shown in Fig. 2a; for mechanical compaction following a given porosity–depth relation we can calculate the relative contribution C_r to the observed foreland sediment thickness due to compaction of underlying extensional basin sediments:

$$C_r = \frac{z_{fo} - z_f}{z_{fo}} \times 100\% \quad (1)$$

When a solidity–depth relation (solidity (S); the complement of porosity) is adopted for normal shale as given by Baldwin and Butler [17]:

$$z = kS^c \quad (2)$$

with $k = 6.02$ km and $c = 6.35$, then the following relation can be derived:

$$C_r = \frac{\left[(1 + z_r)^b - z_r^b\right]^{1/b} - 1}{z_r}; \quad z_r = \frac{z_{fo}}{z_e}$$

$$b = 1 + 1/c \quad (3)$$

Figure 2b illustrates how C_r is controlled by the ratio of observed foreland basin sediments and extensional basin sediments z_r and Fig. 2c shows a contourplot for C_r for several values of z_{fo} and z_e. Both figures demonstrate that, at foreland basins, C_r can reach values of the order of 50% ($z_r = 1/30$), specially when the thin veneer of foreland basin sediments at the cratonward side of the basin overlies thick extensional basin strata.

A third contribution to the accommodation space for foreland basin sediments is due to ongo-

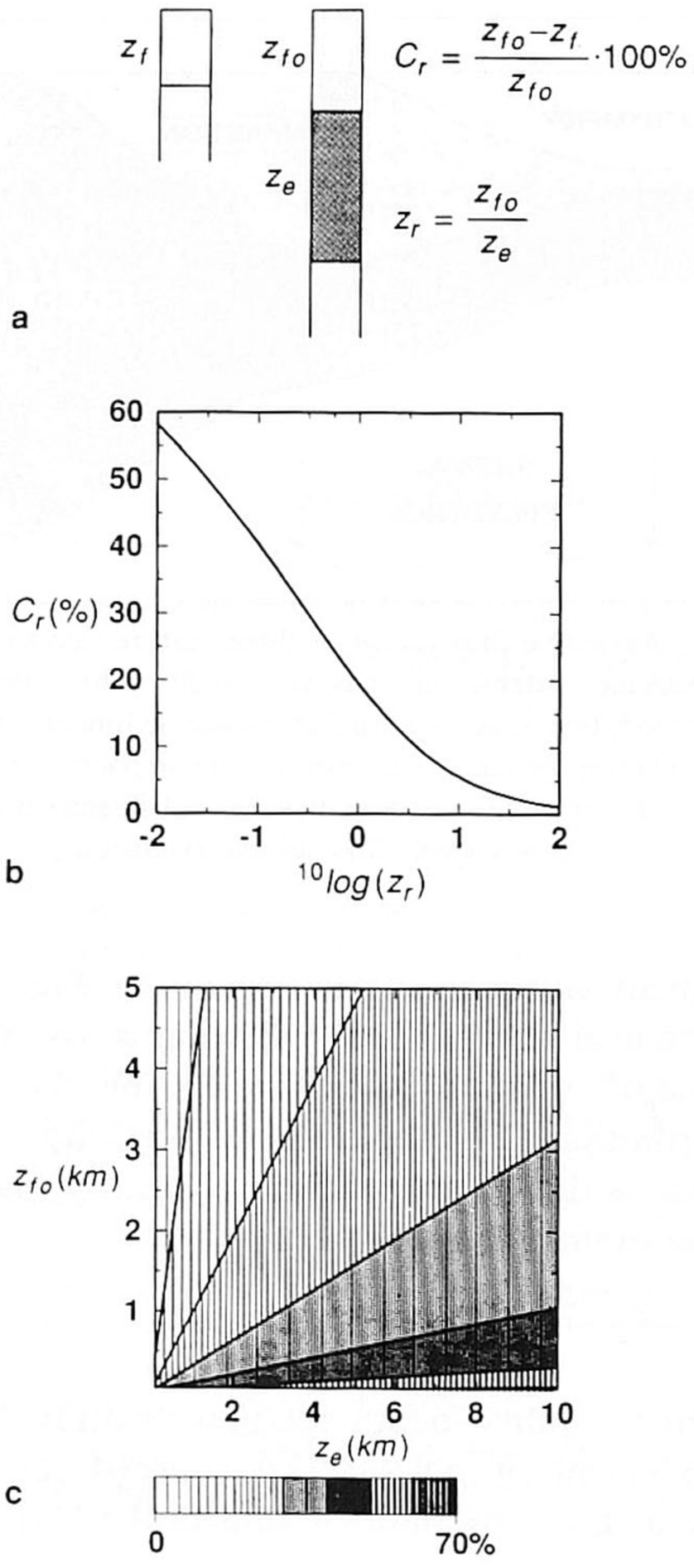

Fig. 2. Relative contribution of compaction of pre-orogenic sediments to accommodation space for foreland basin sediments. (a) Definition of variables: z_{fo} and z_e are observed thicknesses of foreland basin sediments and extensional basin sediments, respectively, and z_r their ratio; z_f is thickness of foreland basin sediments in absence of underlying compacting sediments; C_r is relative contribution to z_{fo} due to compaction of underlying sediments. Compaction calculations for normal shale following [17]. (b) C_r as a function of z_r. (c) Contour plot of C_r as a function of z_{fo} and z_e. Shading is for 10% intervals. Note that thin foreland basin sediments z_{fo} overlying thick extensional basin sediments z_e (i.e. small z_r) can be largely the result of compaction of extensional basin sediments.

ing thermal subsidence induced by the pre-orogenic phase of extension. This contribution is especially of importance when the time span between the rifting phase and the onset of thrust loading is relatively short (i.e. shorter than the thermal time constant of the lithosphere, which is of the order of 60 Ma). A high transient heat content of the lithosphere due to extension also contributes to significant thermal subsidence rates during the foreland basin stage. Such a high transient heat content, in turn, is dependent on the magnitude of lithospheric stretching. High stretching factors β [18], such as at the oceanward side of rifted continental margins, fortify thermal subsidence. Thus, finally, also the location and orientation of the extensional basin with respect to the foreland basin area are important for the contribution of ongoing thermal subsidence to foreland basin subsidence.

2.2. *Effect of extension on flexural rigidity*

Studies of flexure in response to seamount loading and subduction in the oceanic domain have established that the flexural rigidity of oceanic lithosphere is controlled by the thermal state of the lithosphere [19]. The rheology of continental lithosphere is much more complicated than oceanic rheology. Intrinsically, continental lithosphere is relatively weak compared to oceanic lithosphere, due to its rheological stratification [20, 21]. For a pure elastic plate rheology, arbitrarily high stress levels can be supported and an elastic plate is therefore characterized by an infinite strength. By contrast, for oceanic or continental depth-dependent rheology, bending stresses and hence the bending moment are limited by brittle and ductile yield criteria. Consequently, the strength of continental or oceanic lithosphere is finite, which is expressed at sufficiently high stress levels in the failure of the lithosphere. However, reduction of flexural rigidity is already operative at any level of intraplate or bending stress. Furthermore, continental lithosphere due to its often complex petrological composition can contain weakness zones, which can act as detachment horizons, thereby further reducing the flexural rigidity [22, 23]. In spite of these mechanical complexities, especially for continental lithosphere, thermal control on flexural rigidity is similar to oceanic lithosphere. At the same time, modelling studies of flexure at sedimentary basins in response to sediment loading [24] have also confirmed that the flexural rigidity of continental lithosphere following rifting is thermally controlled. Hence, a pre-orogenic phase of extension

is expected to influence the flexural response of the lithosphere on both nappe and sediment loading during the foreland basin stage [see also 25] and might consequently have an expression in the stratigraphy.

3. Thermo-mechanical evolution of the Aquitaine basin

3.1. Tectonic setting

Table 1 schematically summarizes the timing of tectonic events in the Aquitaine basin. The Aquitaine foreland basin is underlain by a Mesozoic rifted basin that was initiated in the early Mesozoic in relation with the Tethyan rift system [26]. This initial extension phase was followed by a minor phase of Kimmeridgian extension that separated the Parentis and the Adour–Mirande sub-basins (Fig. 3a). The Kimmeridgian extension also induced deposition of sediments of fairly uniform thickness over a wide area. A subsequent quiescence period was followed by renewed rifting activity in the Barremian, Aptian and probably also the Albian, contemporaneously with the opening of the Bay of Biscay. This period of rifting is characterized by block-faulting and extremely high subsidence rates in relatively restricted depocentres (the Parentis and Arzacq basins; Fig. 3a) and sinistral movements of Iberia with respect to Europe were probably associated with a belt of pull-apart basins [27, 28]. In the Late Cretaceous, convergence of Iberia and Europe commenced. During Cenomanian–Turonian times, compression started in the eastern part of the Pyrenees [29] after which thrust loading propagated progressively to the western part of the Pyrenees until the Oligocene [30]. The period of time between the

TABLE 1

Timing of tectonic events in the area of the Aquitaine basin

AGES		My.	MAIN EVENTS
Quaternary Neogene		24-0	Post compressive phase: unflexing
Paleogene	Oligocene	36-24	
	Eocene	58-36	Main phase of compression in the western part of the basin
	Paleocene	66-58	
Cretaceous	Late Senonian	84-66	Propagation of the flexuration westward
	Early Senonian	88-84	
	Turonian Cenomanian	98-88	Beginning of the compression in the eastern part of the Pyrenees
	Albian	113-98	Strike slip faulting in the Adour-Mirande Sub-Basin
	Aptian	119-113	Rifting in the 2 Sub-Basins
	Barremian Neocomian	144-119	
Jurassic	Kimmeridgian	156-144	Initiation of the 2 Sub-Basins
		204-156	
	Early Lias	208-204	
Trias		245-208	
Permian			Initiation of the Aquitaine Basin

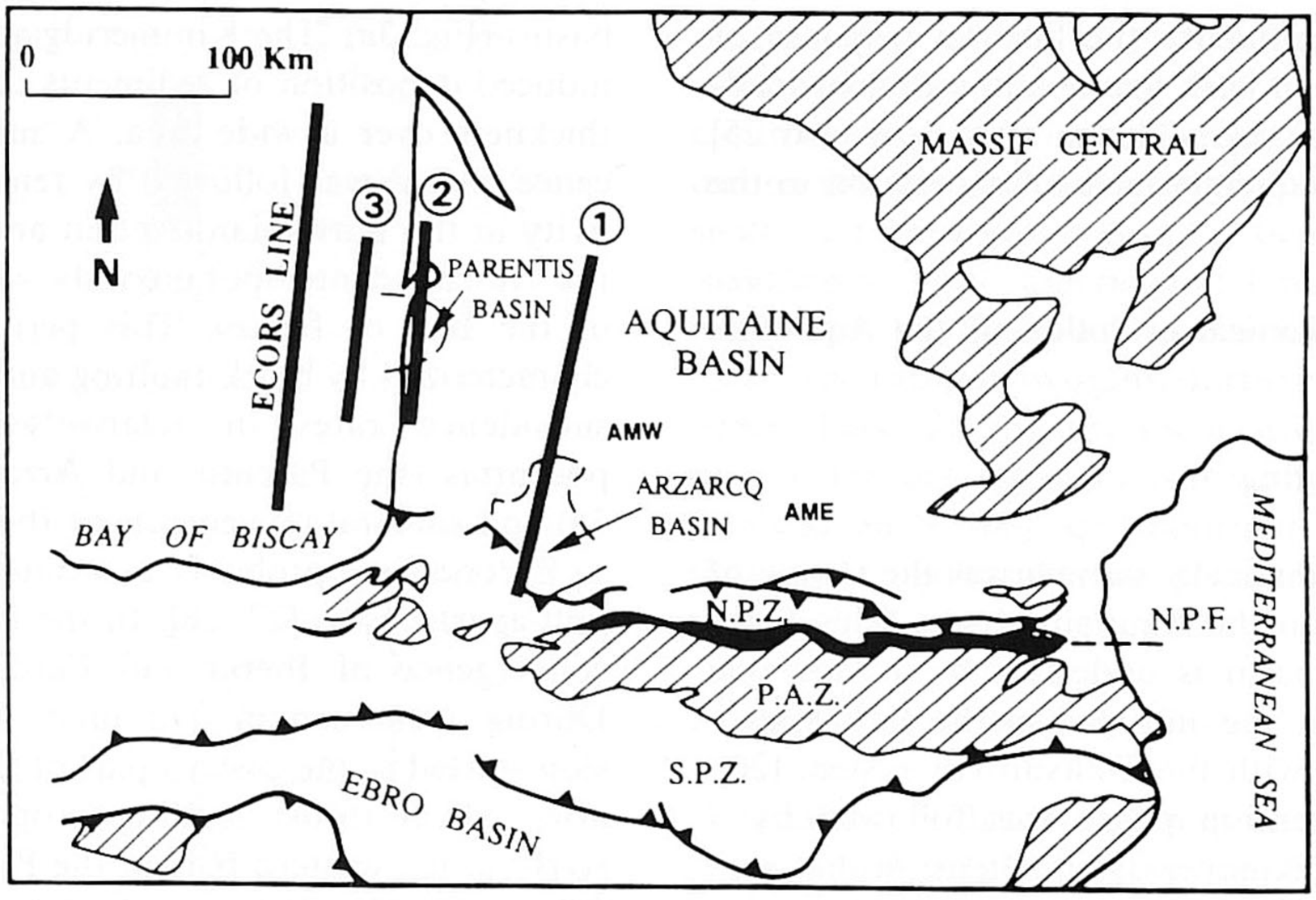

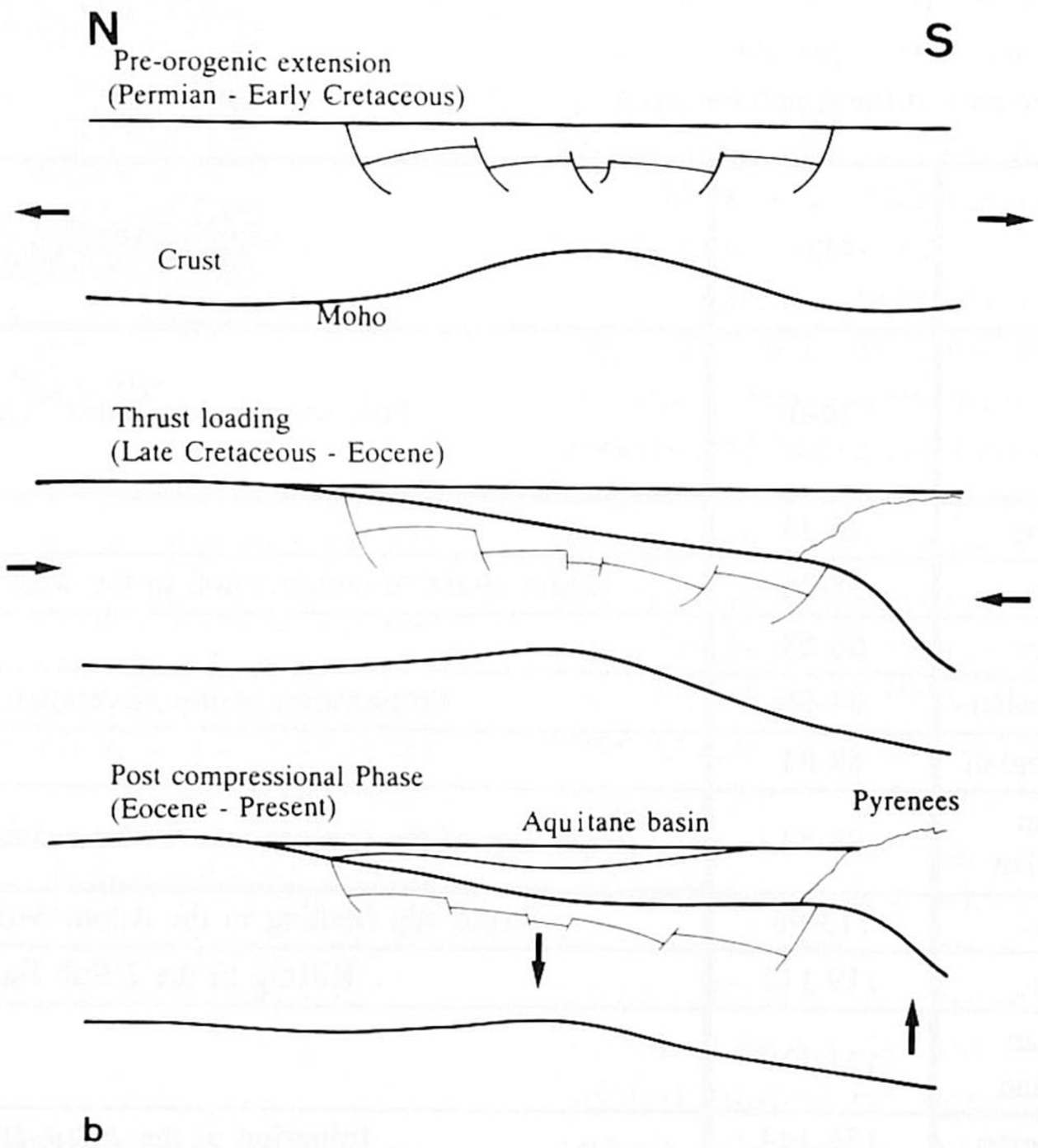

Fig. 3. (a) Map of the Aquitaine basin and surroundings showing the approximate positions of the Parentis and Arzacq sub-basins and the locations of the profiles used in the modelling. Profile 1 across the Arzacq basin is used to constrain the modelling of the pre-orogenic extension period and the period of foreland basin evolution. Profiles 2 and 3 traversing the Parentis basin are used in modelling of the extension period only. *NPZ*: North Pyrenean Zone; *NPF*: North Pyrenean Fault; *PAZ*: Pyrenean Axial Zone; *SPZ*: South Pyrenean Zone. *AMW* and *AME* denote the western and eastern part of the Adour–Mirande sub-basin, respectively. (b) Schematic evolution of the Aquitaine domain. Above: (Permian–Early Cretaceous) pre-orogenic extension phase; rifting of the European domain. Middle: (Late Cretaceous–Eocene) compression; formation of the Aquitaine foredeep. Below: (Eocene–Present) post-compressive phase associated with unflexing.

end of extension and the onset of the compressional period is, therefore, of the order of only 10 Ma. During the post-deformation phase of the Pyrenean orogeny, erosion of the overthrust loads and of large parts of the basin has been observed, contemporaneous with sedimentation and in more distal parts of the basin [31, 32]. During this so called period of 'unflexing', sedimentation was only significant in the western part of the Aquitaine basin. Figure 3b schematically summarizes the tectonic evolution of this region.

3.2. Phase of extensional tectonics (156–98 Ma)

We have analyzed three cross-sections (Fig. 3a), using a stretching model of basin subsidence [18, 33]. Two of these sections cover the onshore and offshore parts of the Parentis basin, the former being parallel to the ECORS deep seismic profile [34]; the third section is chosen perpendicular to the Pyrenean fold belt, crossing the Arzacq basin. We have incorporated lateral variation of stretching parameters β, multiple stretching phases with a finite duration [35], lateral heat flow [36] and the effects of lateral and temporal changes of flexural rigidity (Appendix 1) (see also [37]). We have used paleobathymetry estimates from Mathieu [38] and Brunet [39]. Compaction of sediments has been accounted for by using an exponential porosity–depth relation [40] with a surface porosity and characteristic depth constant chosen to fit porosity-data from the Parentis basin: $\Phi(z) = 38\ e^{-0.41z}$.

TABLE 2

Stretching factors Arzacq basin model (Fig. 5a)

Position (km)	β (156–144 Ma)	β (119–98 Ma)	β (total)
405	1.10	2.20	2.42
420	1.10	2.20	2.42
430	1.10	1.43	1.57
440	1.10	1.32	1.45
450	1.10	1.21	1.33
460	1.10	1.12	1.23
470	1.10	1.05	1.16
480	1.10	1.00	1.10
600	1.10	1.00	1.10
610	1.00	1.00	1.00

We have constructed the stratigraphic section through the Arzacq basin from BGRM et al. [41] isopach maps (Fig. 4). For the modelling, the southern part of the Arzacq basin, which has been overridden and deformed during the Pyrenean orogeny, has been reconstructed by symmetrical extension of the basin north of the North Pyrenean Fault to the south. We have employed both a Kimmeridgian/Portlandian (156–144 Ma) and an Aptian/Albian (119–98 Ma) stretching phase. Total crustal thinning values were estimated from Moho depth data [42] and depth estimates for the top of the Paleozoic [41]. We have tested several rigidity models (constant effective elastic thicknesses (EET) and EET's controlled by the depth to various isotherms) in combination with various total β-estimates (keeping within the bounds set

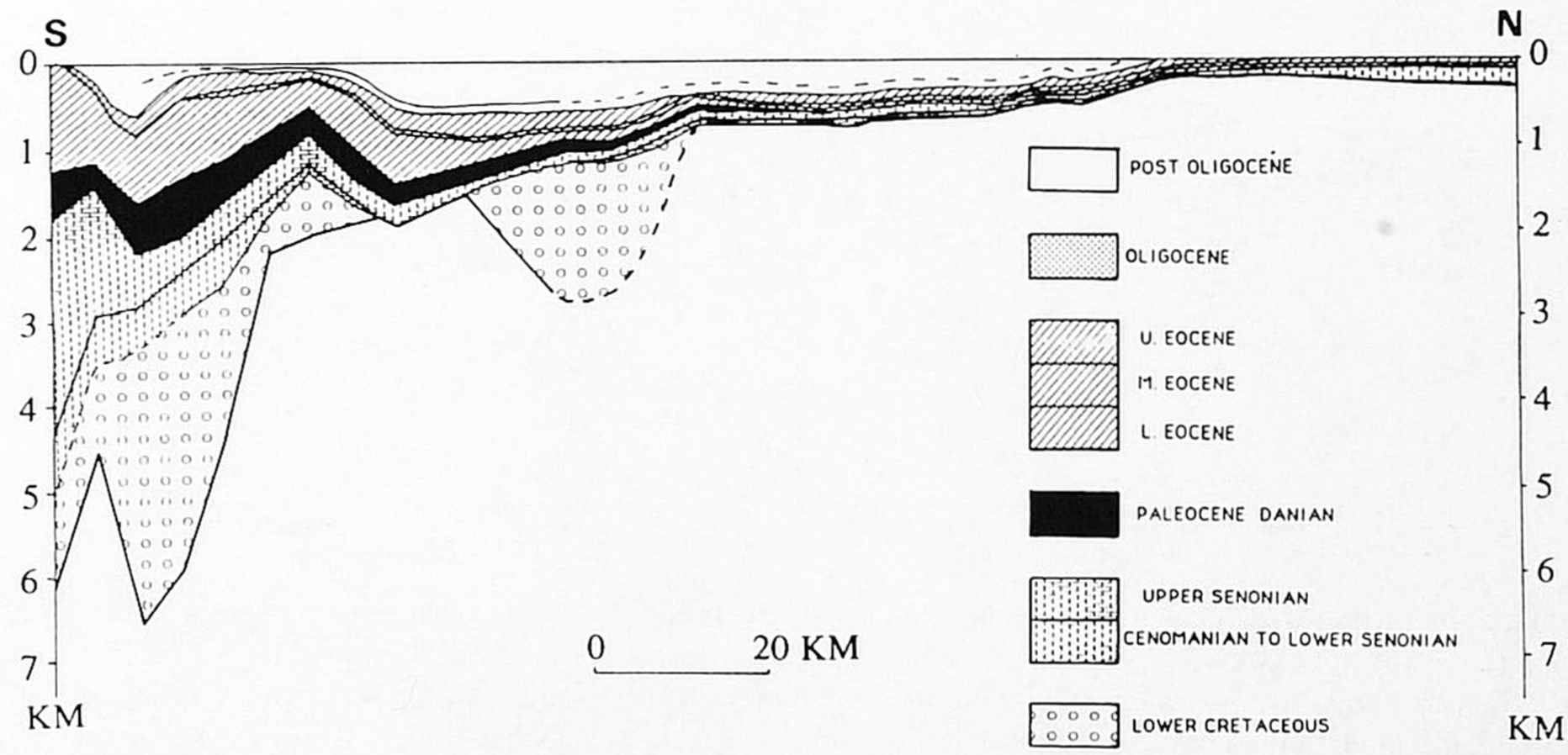

Fig. 4. Stratigraphic section across the Arzacq basin (cross-section 1 in Fig. 3a), constructed from BGRM et al. [41] isopach maps.

for crustal thinning), and obtained the best fit for a total β of 2.42 (Table 2) and an EET of approximately 15 km (isotherm controlled; Fig. 5). This rigidity estimate is in accordance with findings by Brunet [43] and Desegaulx et al. [31]. Table 3 shows a comparison of averaged thickness data and predictions from the modelling. Figure 5b shows a comparison of the pre-Eocene subsidence data and the model predictions. The Paleocene sediment thickness seems to be overestimated, which is probably the result of uncertainties in paleobathymetry. In contrast, the predicted Eocene sediment thickness is too small by a factor three, because the modelling ignores Pyrenean thrust loading and flexing of the lithosphere at that time. The subsequent post-orogenic subsidence evolution of the foreland basin stage is depicted in Fig. 5c.

For the profiles crossing the Parentis basin we obtain similar results. We have tested two tectonic scenarios that share a common Kimmeridgian/Portlandian stretching phase (156–144 Ma), but that differ in the timing (Barremian/Aptian (124–113 Ma) or Barremian/Aptian/Albian

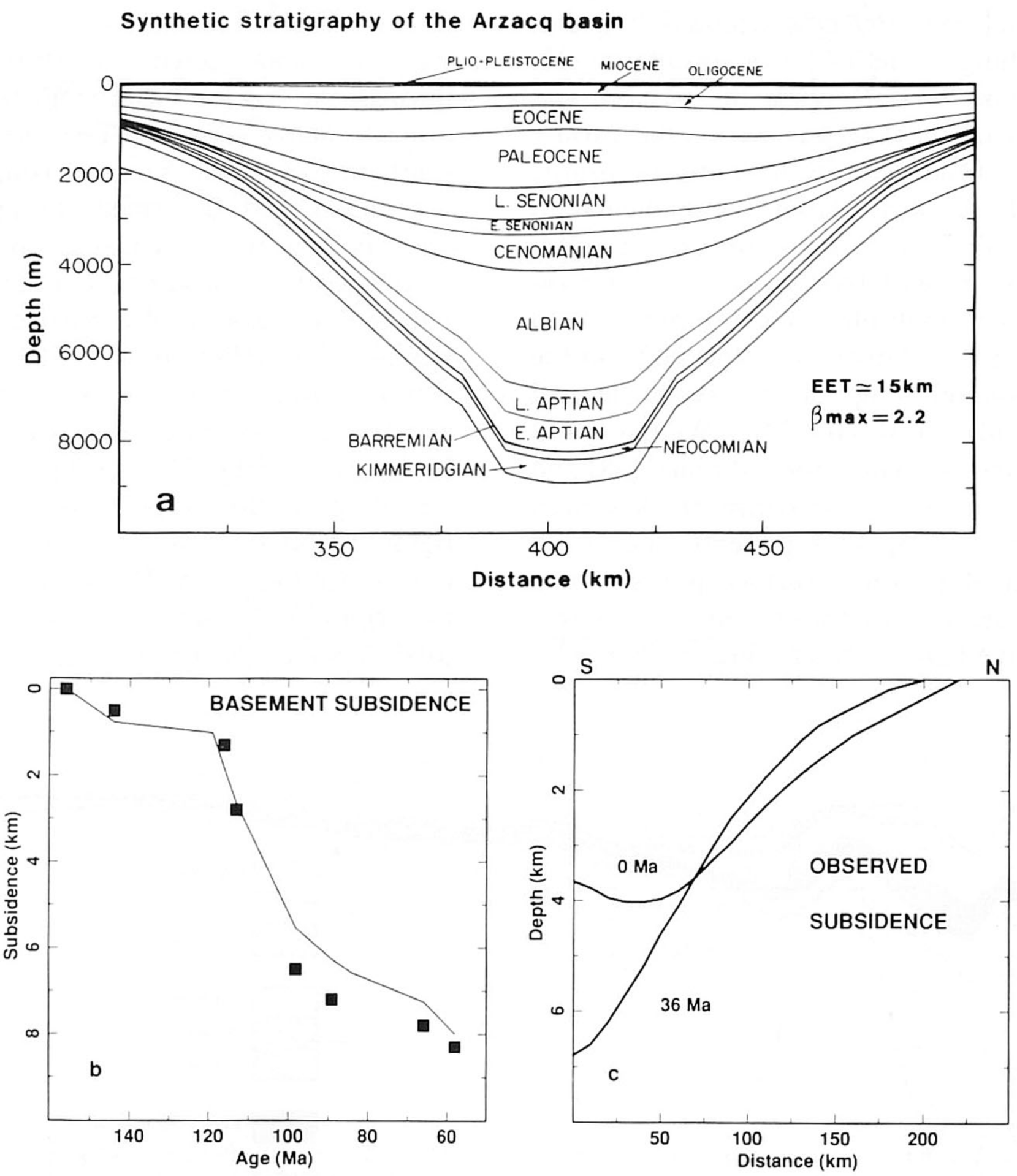

Fig. 5. (a) Stratigraphy of the Arzacq basin predicted by the stretching model (stretching factors are given in Table 2). A low effective elastic thickness (EET), of approximately 15 km is required to reproduce the overall stratigraphic pattern (Table 3). The basin north of the North Pyrenean Fault (Fig. 4) has been symmetrically extended to the south. (b) Comparison of basement subsidence data (squares) and synthetic model predictions (solid line). (c) Tectonic basement subsidence for the section crossing the Arzacq basin for the early-Oligocene and the present-day situation. The curves demonstrate the post-orogenic unflexing phase (modified after [30]).

(124–98 Ma)) of the Early Cretaceous stretching phase. Constraints for β-values are derived from the Bay of Biscay ECORS line with a $\beta = 4.5$ as a maximum crustal thinning value in the centre of the basin. The best fit to the Lower Cretaceous stratigraphy is obtained for an Early Cretaceous stretching phase that is restricted to Barremian/Aptian times only. This indicates that the thick sequence of Albian deposits, particularly present in the off-shore part of the Parentis basin, was probably not deposited in response to active Albian stretching, but is mainly the result of rapid infilling of a Late Aptian deep water basin. As for the Arzacq basin, the inferred EET underlying this basin was found to be very low (approximately 10 km). Here, we ignore possible mechanical complexities for the flexural rigidity associated with continental rheology (as discussed above) and employ the isotherm definition of flexural rigidity to estimate the relative impact of the thermal perturbation resulting from pre-orogenic extension. Figure 6 illustrates the evolution of the EET for the Arzacq basin. Variation of the values of β between uncertainty limits, and using different isotherms to define the EET do not affect the overall pattern of the temporal evolution of EET, which shows a reduction in thermally defined EET

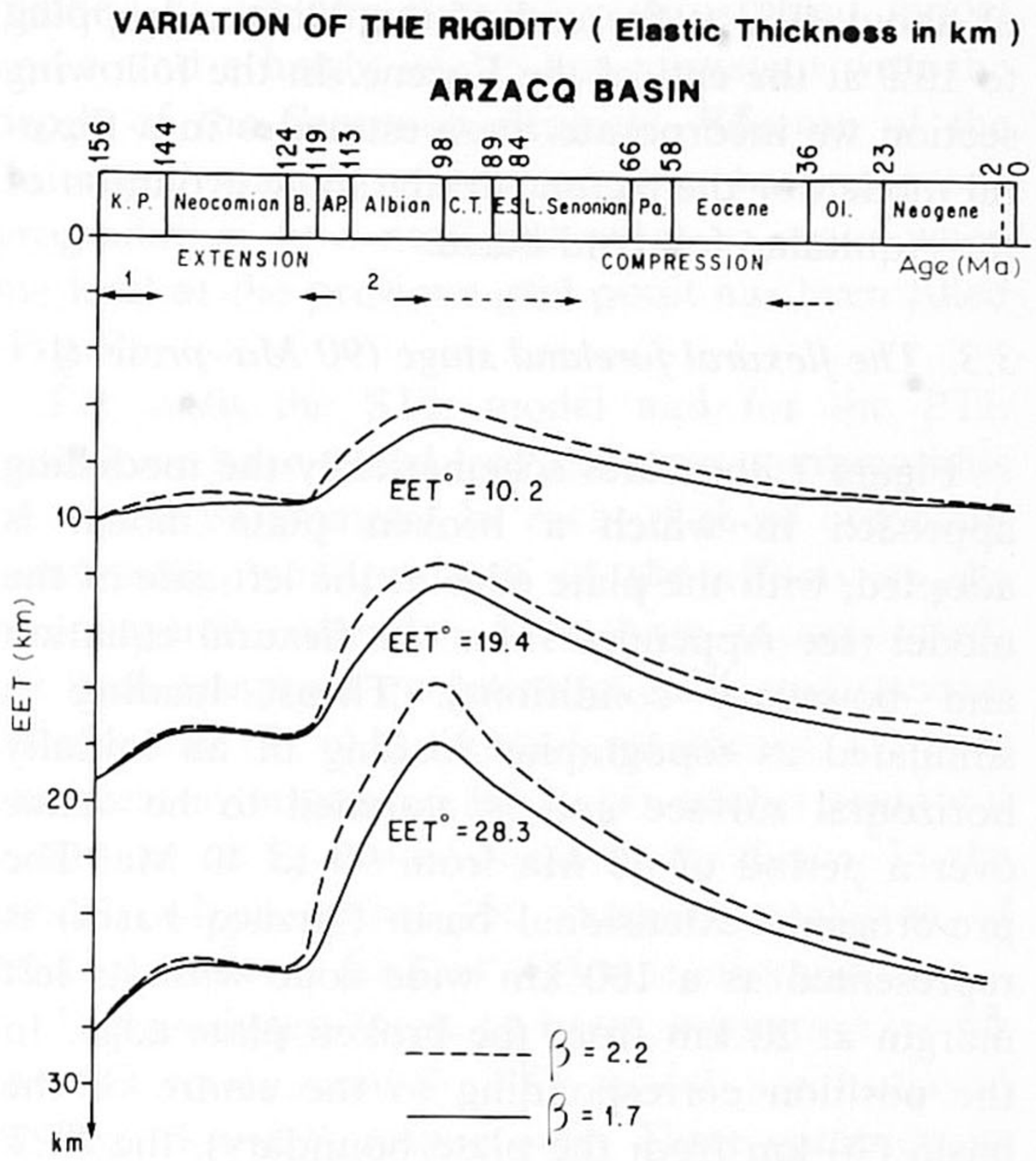

Fig. 6. Models for the temporal evolution of EET for the Arzacq basin, as predicted by the depth of several isotherms and two Aptian/Albian β-values. These results demonstrate that the EET at the end of the Albian has dropped to about 60% of its original value and gradually increases during and following the compressive phase. EET^0 denotes the EET prior to stretching.

TABLE 3

Comparison of estimates for observed, and predicted maximum sediment thickness for the Arzacq basin for several time slices

AGES	DATA	MODEL
Late Eocene	200	600
Middle Eocene	500	
Early Eocene	1000	
Paleocene	700	1300
Late Senonian	600	700
Cenomanian Early senonian	>600	1150
Albian	3500	2800
Late Aptian	1500	1400
Early Aptian	800	
Barremian		100
Neocomian		150
Kimmeridgian Portlandian	500	550

of about 40% at the end of the Albian, dropping to 10% at the end of the Eocene. In the following section we incorporate these estimates in a flexural model for the tectonostratigraphic evolution of the Aquitaine foreland basin.

3.3. The flexural foreland stage (90 Ma–present)

Figure 7 illustrates schematically the modelling approach in which a broken plate model is adopted, with the plate edge at the left side of the model (see Appendix 1 for the flexural equation and boundary conditions). Thrust loading is simulated as topographic loading of an initially horizontal surface and is assumed to be active over a period of 50 Ma from 90 to 40 Ma. The pre-orogenic extensional basin (Arzacq basin) is represented as a 100 km wide zone with its left margin at 20 km from the broken plate edge. In the position corresponding to the centre of the basin (70 km from the plate boundary), the EET evolves through time from 14 km at the beginning of the compressive phase to 20 km at 40 Ma after the cessation of thrust loading. This temporal evolution of EET is assumed to decrease linearly to the basin margins, which have been assigned a constant value of 20 km. In the flexural calculations, we assume that the temporal increase in EET is only of significance for newly emplaced loads, or, alternatively, that the deflections due to previously emplaced loads are not affected by subsequent changes of EET. This assumption is based on flexure studies of oceanic lithosphere in response to seamount loading. The results of these studies are consistent with the idea that the age and hence strength of the lithosphere at the time of loading controls the response to loading, as opposed to the present age/strength of the litho-

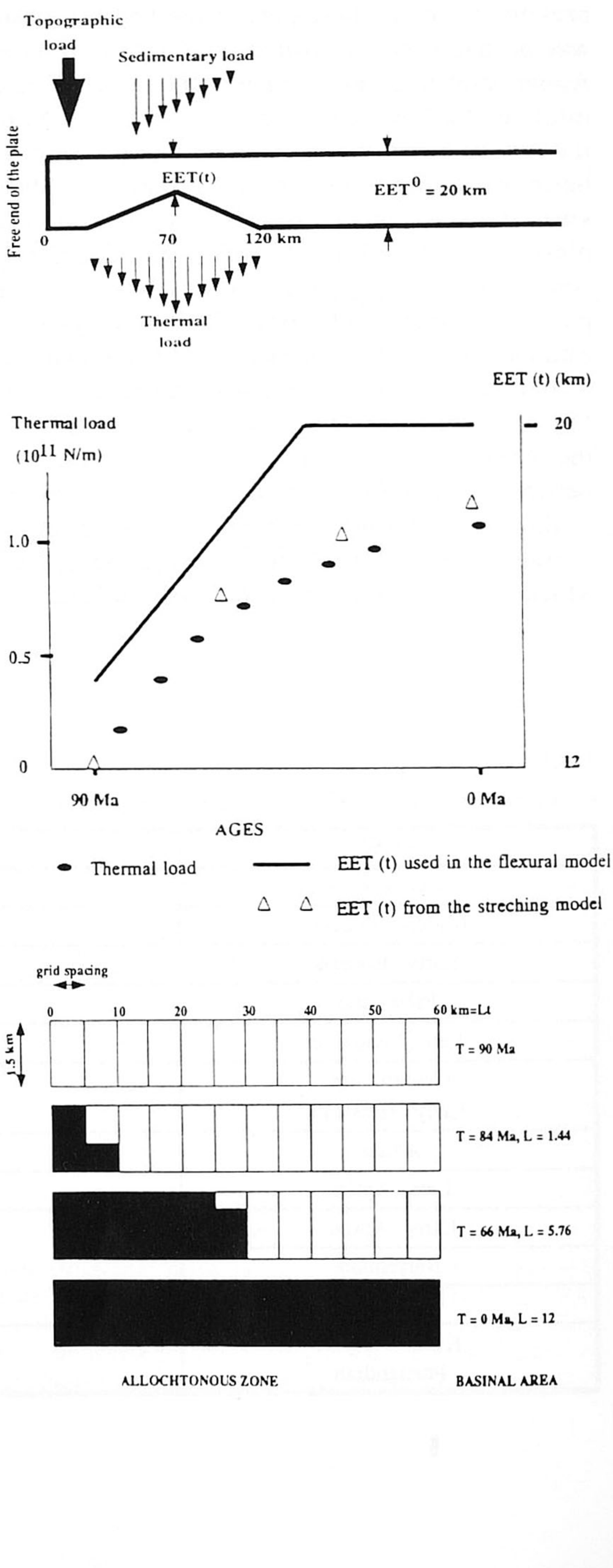

Fig. 7. Schematic illustration of the model used to study the effect of extensionally induced attenuation of flexural rigidity and ongoing thermal subsidence on foreland basin subsidence. Above: the model employs a semi-infinite elastic plate with either a constant uniform plate thickness EET^0, or a thinned plate EET(t) between 20 and 120 km. The thermal load is also applied between 20 and 120 km. Topographic (thrust) loading occurs over a period of 50 Ma (90–40 Ma). Stationary thrust loading is applied at 25 km and the prograding thrust loading between 0 and 60 km (see lower part of figure). Middle: the triangles denote the change of plate thickness through time (EET(t)) for the centre of the pre-orogenic basin, 70 km from the plate edge, from the extensional basin modelling. The continuous line is the same, as used in the foreland basin modelling. The dotted line denotes the thermal loading history employed in the modelling. Below: illustration of the linear thrust load progradation over the 60 km wide allochthonous zone as applied in the prograding thrust load modelling. Note the discrete steps, inherent to the finite difference technique.

sphere (e.g. [19]). The ongoing thermal subsidence of the basin is represented by a vertical load force distribution with its maximum located at the centre of the basin and which linearly decreases to zero at the basin margins. The magnitude of this force has been calculated from the extensional basin modelling (see Appendix 2). Note that, inherent to this approach, the assumption is made that the compressive phase does not influence the thermal state of the lithosphere. The space created by both thrust loading and thermal subsidence is filled with sediments up to sea level. In the present modelling, we concentrate on the consequences of thermal subsidence and the temporal evolution of EET. The contribution to the accommodation space for foreland basin sediments due to compaction of pre-orogenic sediments and infill of pre-orogenic bathymetry, as discussed above, have been ignored in these models. It is therefore important to realize that our predictions of foreland basin sediment thicknesses provide underestimates. The onlap relations predicted by the models, however, are not significantly affected by compaction or infill of pre-existing bathymetry. We have adopted a constant density of 2500 kg m^{-3} for the sediments and a density of 3200 kg m^{-3} for the displaced mantle or asthenosphere material.

We have investigated two scenarios for the topographic loading history; a stationary thrust load (STL) model and a more realistic prograding thrust load (PTL) model.

In the STL model, we assume a point load located at 25 km from the broken edge of the plate. The magnitude of this load has been obtained by requiring a depth of 3.5 km for the base of the Senonian series (onset of compressional events) in the autochthonous foreland basin as observed in Fig. 4. For a thrust load density of 2700 kg m^{-3}, this point load is equivalent to a box 5 km wide (corresponding to the grid spacing in the flexural calculations) and a height which linearly increases from 90–40 Ma up to a value of 15 km.

In the PTL model, we have assumed a linear progradation in time of the topographic load from the plate edge over a distance of 60 km (Fig. 7). This distance of progradation is in accordance with reconstructions of the allochthonous domain in the Pyrenees [44]. For the magnitude of the thrust load, we have used the same calibration method as for the stationary thrust load model and found a height of 1.5 km consistent with the depth of the Senonian deposits. Because of the finite grid spacing in the model, we have imposed progradation to a new grid point to occur when the load at the previous grid point has been filled (Fig. 7).

For both the STL model and for the PTL model, we have tested four different combinations of model parameters. In each of these combinations none, one or both of the effects of the pre-orogenic extension have been incorporated: (1) both temporal evolution of EET and thermal subsidence; (2) only thermal subsidence; (3) only temporal evolution of EET; (4) neither temporal evolution of EET nor thermal subsidence. In the models which ignore the temporal evolution of EET, a constant EET of 20 km is adopted.

The predicted foreland basin stratigraphies for the STL models and the PTL models are displayed in Figs. 8 and 9, respectively. Three conspicuous features are present which characterize the differences between the eight models: the total basin depth, the amount of post-orogenic sediments and the length of basement onlapping of strata. Comparison of the figures demonstrates that the predicted basin depth is about 40% larger for the models which account for ongoing thermal subsidence. The same models are the only models associated with Oligocene, Neogene and Quaternary post-orogenic sediments due to the ongoing creation of accommodation space after thrusting activity has ceased. In all models which incorporate ongoing thermal subsidence, the predicted thickness of the post-orogenic sediments is approximately 200 m. This value is somewhat lower than the 400 m of post-Eocene sediments encountered in the exploration well Clermont H-1, located just west of the studied cross-section. Inspection of Fig. 2 shows that for compaction to account for this discrepancy, at least 12 km of pre-orogenic sediments should underly the Aquitaine basin. Such a thickness is not present, however. Salt-tectonics locally may have significantly contributed to the post-orogenic subsidence, but can probably not be invoked to account for 200 m of subsidence over the entire basin. The contribution of ongoing thermal subsidence to the thickness of the strata is largest during the earliest phases of foreland basin sedimentation and gradually de-

creases towards the present. The models which incorporate a temporal evolution of EET, consistently predict about 1 km more subsidence beneath the allochthonous foreland basin close to the plate edge relative to the constant EET models. By contrast, in the autochtonous foreland basin, for these models, the basin depth is shallower than for the constant EET models. This effect, which is the result of the position of the modelled foreland basin relative to the broken edge of the plate, is illustrated in Fig. 11. Note, however, that the stratigraphies shown in Figs. 8 and 9 do not display the allochthonous foreland basin to the left of the 60 km position (see inset Figs. 8a and 9a), so that only the minor shallowing of this part of the basin for the models incorporating a temporal evolution of EET can be observed in these figures.

For the STL models, significant basement onlapping (minimum 5 km) is only observed for the model including both temporal evolution of EET and thermal subsidence (Fig. 8a). The length of basement onlapping is much larger for the PTL models. Especially when thermal subsidence is ignored (Fig. 9, c and d), the length of basement onlapping is of the order of the distance of thrust load progradation (60 km) and is clearly enhanced by the temporal evolution of EET. Conversely, ongoing thermal subsidence reduces the distance of basement onlapping (Fig. 9, a and b). This is

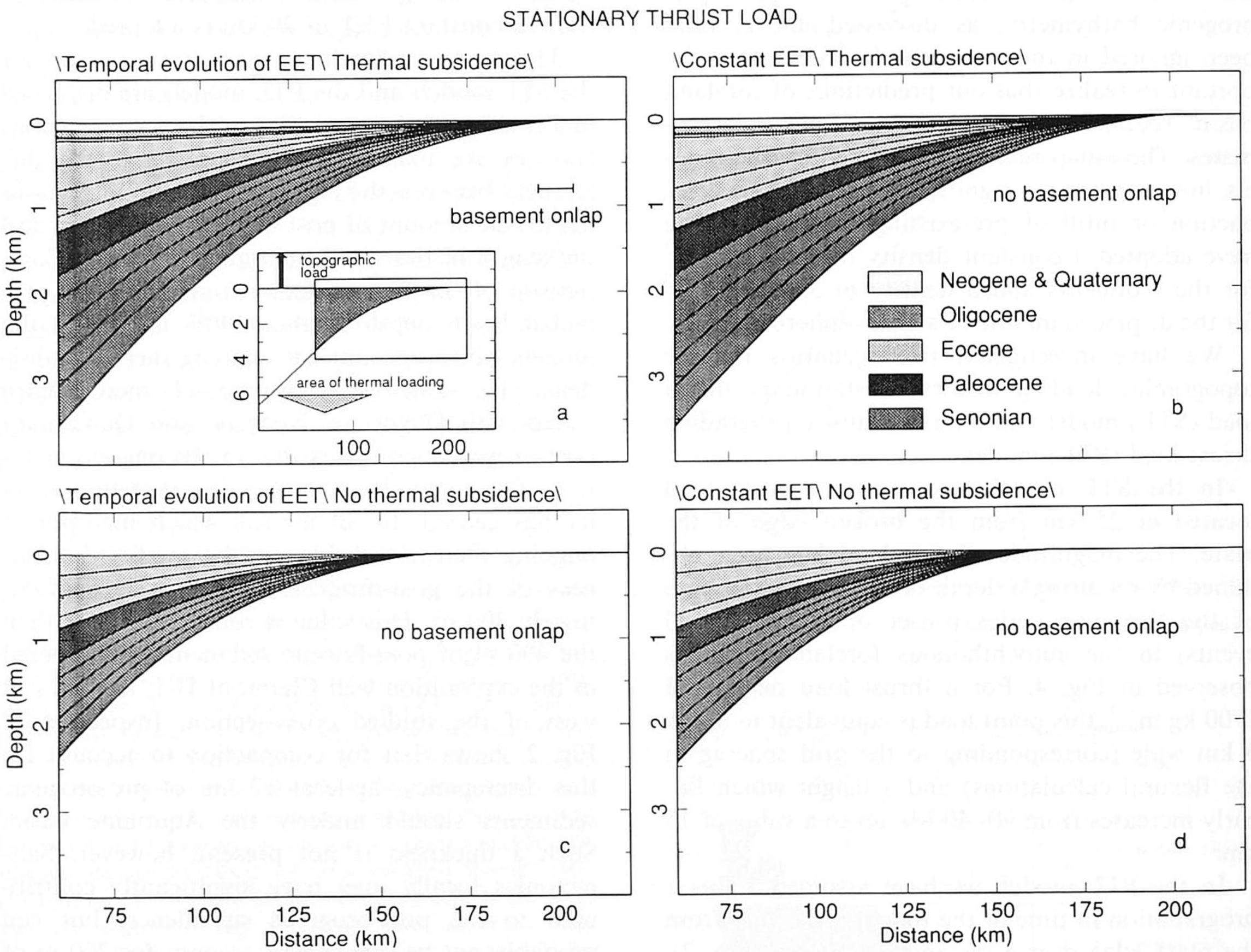

Fig. 8. Stratigraphic predictions for the stationary thrust load (STL) models (see inset in a). The arrow denotes the direction in which the thrust load is increasing through time. Chronostratigraphic horizons are given for Senonian (90, 84, 80, 75, 70, 66 Ma), Paleocene (58 Ma), Eocene (55, 50, 45, 40, 36 Ma), Oligocene (24 Ma) and Neogene–Quaternary (0 Ma). (a) Model incorporating both temporal evolution of EET and ongoing thermal subsidence. (b) Constant EET; ongoing thermal subsidence. (c) Temporal evolution of EET; zero thermal subsidence. (d) Constant EET; zero thermal subsidence.

because during the early phase of subsidence, the width of the basin is controlled by the area of thermal subsidence and not by the location of thrust loading. Ongoing thermal subsidence also results in the area of onlap being located farther from the thrust front. 25 km of basement onlapping is predicted for the most realistic and most complete model which incorporates prograding thrust loading, ongoing thermal subsidence and a temporal evolution of EET (Fig. 9a).

Figure 10 documents observed basement onlapping in the Aquitaine basin from Cenomanian to Lower Eocene times. This onlapping pattern has been compiled from BGRM et al. [41] isopach maps. Since the true cratonward pinch-outs of the strata are rather uncertain, we approximated the pattern of basement onlapping by iso-lines of a fixed sedimentation rate of 14.3 m Ma^{-1} (corresponding to 200 m of deposits for the Cenomanian–Early Senonian period). These iso-sedimentation-rate lines show that significant cratonward shift of basement onlap is present in the Aquitaine basin, and that the pattern of onlapping is laterally variable. Cenomanian–Early Senonian deposits are found far north and northwest of the Arzacq basin (see also Fig. 4), but are much less widespread more to the east. This is consistent with the model predictions (Fig. 9a). According to the iso-lines, the Cenomanian–Early Senonian transgression is followed by an Early–Late Senonian regression north of the Arzacq basin. Inspection of Fig. 4 shows that this is probably an artefact of the use of iso-lines of a fixed sedimentation rate, rather than the true zero sediment thickness. A thin veneer of Senonian deposits is present far north of the corresponding iso-sedi-

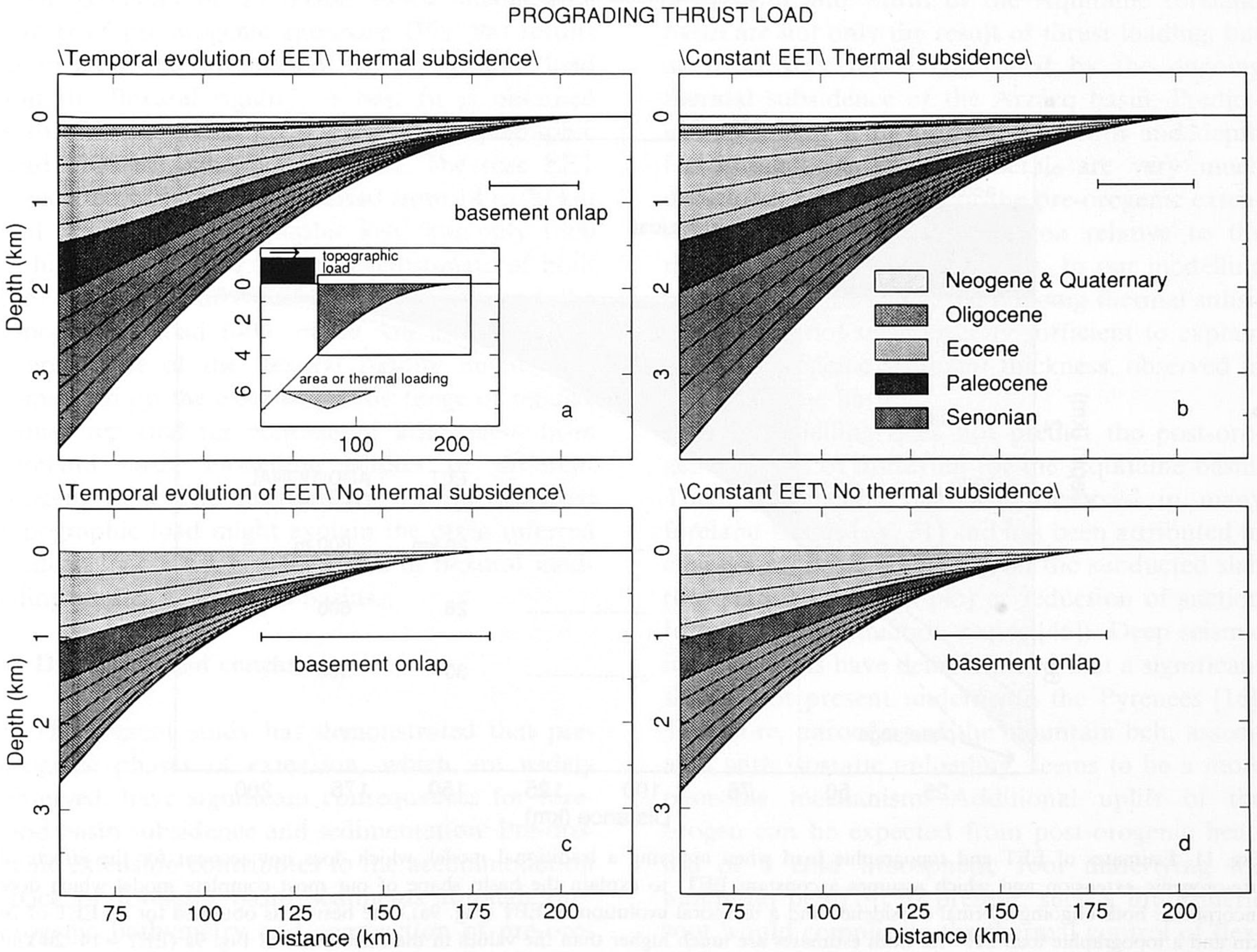

Fig. 9. Stratigraphic predictions for the prograding thrust load (PTL) models (see inset in a). Figure convention as in Fig. 8.

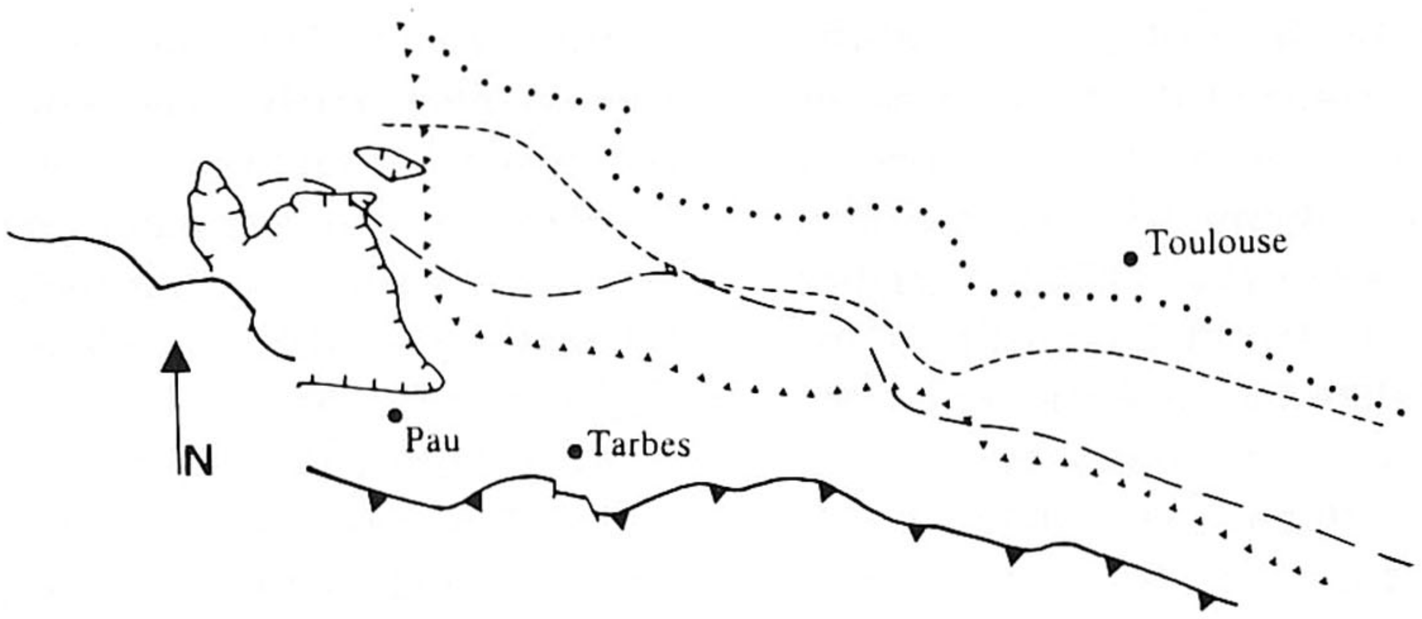

Fig. 10. Map for the Aquitaine basin with lines of constant sedimentation rate (14.3 m/Ma) for several periods from Cenomanian to Lower Eocene times constructed from BGRM et al. isopach maps [41]. Shifts in these lines approximate the temporal pattern on basement onlapping. The northward shift in onlap north and northeast of the Arzacq basin is probably less extensive than more to the east, where significant pre-orogenic extensional basins have not been observed. This is in accordance with the findings of the most complete model of Fig. 9a.

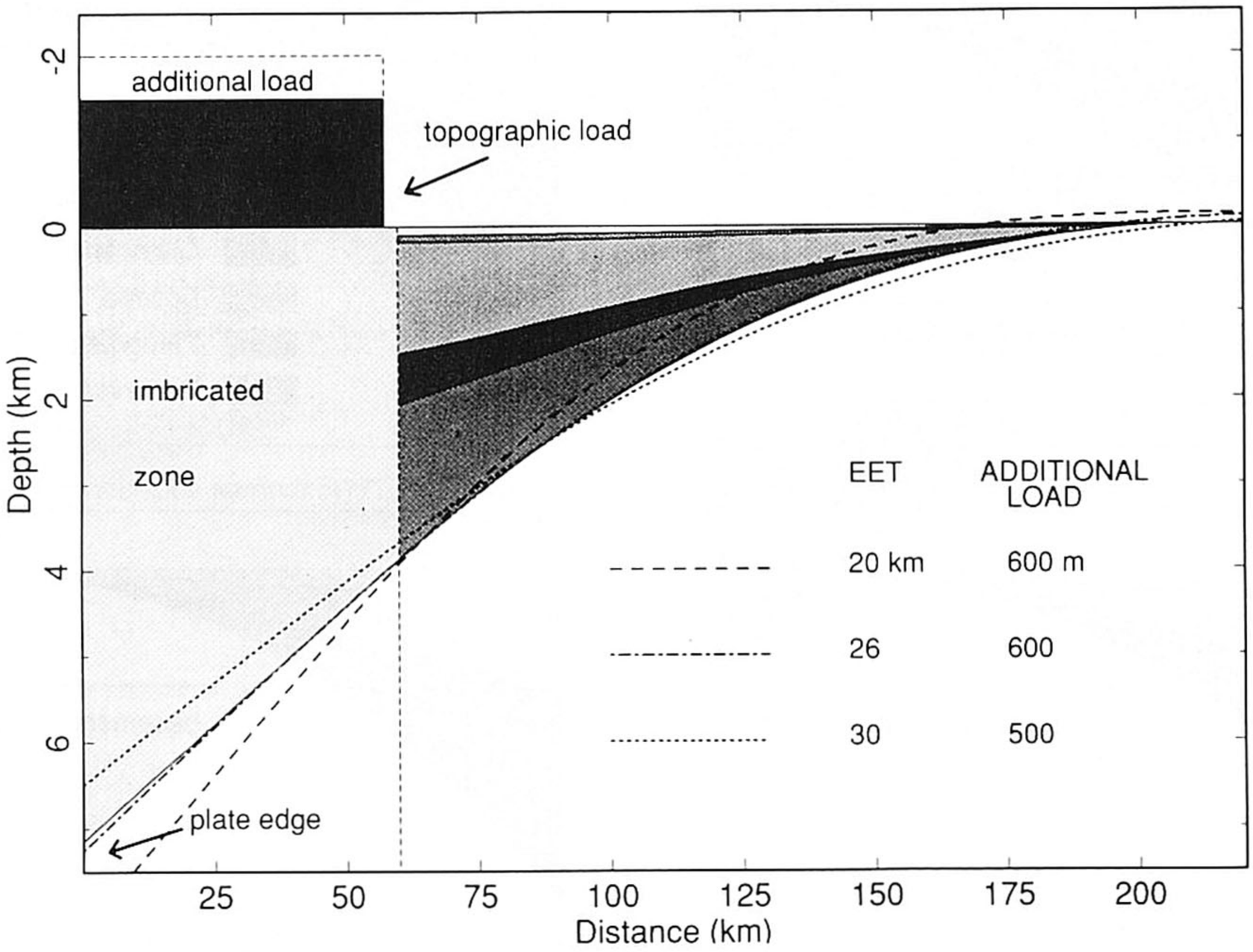

Fig. 11. Estimates of EET and topographic load when applying a traditional model, which does not account for the effects of pre-orogenic extension and which assumes a constant EET, to explain the basin shape of our most complete model which does incorporate both ongoing thermal subsidence and a temporal evolution of EET (Fig. 9a). The best fit is obtained for an EET of 26 km and a topographic load 2100 m. Both estimates are much higher than the values in the calculation of Fig. 9a (EET = 14–20 km; topographic load = 1500 m).

mentation-rate line in Fig. 10. Moreover, the pattern of basement onlapping is probably complicated by variations of paleotopography at the onset of thrust loading and the ongoing subsidence of the Parentis basin (Fig. 3a). In spite of all these complications, the model predictions seem to be at least in qualitative agreement with observations.

The present modelling has demonstrated that the foreland basin evolution of the Aquitaine basin is probably very much affected by the thermomechanical inheritance of pre-orogenic extension phases. The more complete modelling approach, which incorporates these effects (Fig. 9a), predicts a basin geometry and infill architecture very different from the more traditional modelling approach (Fig. 9d), which does only employ topographic loading. Conversely, Fig. 11 demonstrates that applying the more traditional modelling approach of only topographic loading to explain the basin geometry of the model which includes the effects of pre-orogenic extension (Fig. 9a) results in errors in the estimates of the topographic load and the flexural rigidity. A best fit is obtained with a constant EET of 26 km and a topographic load 2100 m high (60 km wide). The true EET associated with the model varied from 14 to 20 km and the original topographic load was only 1500 m high. Hence, a significant overestimate of both the flexural rigidity (30–43% of EET) and the topographic load (40% or 36 km^2) results. The overestimate of the flexural rigidity might shed some light on the extremely wide range of rigidity values reported for continental lithosphere from foreland basin modelling studies of different orogens [20]. The overestimate of the required topographic load might explain the often inferred 'hidden load' or subsurface load in flexural modelling studies at foreland basins.

4. Discussion and conclusions

The present study has demonstrated that pre-orogenic phases of extension, which are widely observed, have significant consequences for foreland basin subsidence and sedimentation. Pre-orogenic extension contributes to the accommodation space of foreland basin sediments through pre-orogenic bathymetry and compaction of pre-orogenic sediments. In addition, the extension-induced transient thermal state of the lithosphere, results in ongoing thermal subsidence, and a flexural rigidity which changes through time. This is especially important when the time span between the end of the phase of extension and the onset of compression is relatively short.

Our modelling has shown that shifting onlap patterns, such as observed for the Aquitaine foreland basin, are probably the result of the complex interaction of advancing thrust sheets, changes of the flexural rigidity of the lithosphere and ongoing thermal subsidence due to pre-orogenic extension phases. For the Aquitaine foreland basin the increase of flexural rigidity associated with the pre-orogenic Arzacq basin enhances significant cratonward shift in basement onlap, whereas the ongoing thermal subsidence counteracts this phenomenon. This results in a net predicted distance of basement onlap which is less than expected in a model which ignores ongoing thermal subsidence. The depth and width of the Aquitaine foreland basin are not only the result of thrust loading, but are also very much controlled by the ongoing thermal subsidence of the Arzacq basin. Predictions of onlap patterns and the width and depth for foreland basins in general, are very much dependent on the width of the pre-orogenic extensional basin and of its position relative to the thrust loads and the plate edge. In our modelling of the Aquitaine basin, the ongoing thermal subsidence does not seem entirely sufficient to explain the post-orogenic sediment thickness, observed in the Aquitaine basin.

Our modelling does not predict the post-orogenic period of unflexing for the Aquitaine basin. This phenomenon has been observed in many foreland basins [e.g. 31] and has been attributed to changes in the forces acting on the subducted slab (e.g. slab detachment [45] or reduction of suction forces when subduction ceases [46]). Deep seismic investigations have demonstrated that a significant slab is not present underneath the Pyrenees [16]. Therefore, unroofing of the mountain belt, associated with isostatic unloading, seems to be a more plausible mechanism. Additional uplift of the orogen can be expected from post-orogenic heating of a cold lithospheric root underlying the mountain belt [14]. If present, such a lithospheric root would complicate the thermal control of flexural rigidity. Moreover, as discussed previously,

the temporal evolution of flexural rigidity may be further complicated by changes in the stress state of the lithosphere. Relaxation of a compressive state of stress in the lithosphere not only reinforces the thermally induced increase in flexural rigidity, but fluctuations in the intraplate stress level or orientation would also induce relative sea-level changes and produce a punctuated stratigraphy [37, 47].

The present study has shown that the inherited thermo-mechanical structure of the lithosphere associated with pre-orogenic extension phases can significantly affect the record of vertical motion and the stratigraphy of foreland basins. Modelling which accounts for these effects, in addition to topographic loading, to explain the basin geometry of foreland basins significantly reduces the estimates of both the flexural rigidity (30–43% for the Aquitaine basin) and the required topographic load (40% for the Aquitaine basin). Emplacement of thrust loads below sea level, as expected in a pre-orogenic extensional basin setting, further reduces the required topographic load. Therefore, pre-orogenic extension might shed some light on the extremely wide range of rigidity values reported for continental lithosphere from foreland basin modelling studies of different orogens [22]. Furthermore, pre-orogenic extension could explain, in many instances, the often inferred 'hidden load' or subsurface load in flexural modelling studies at foreland basins.

Acknowledgements

Partial support for this work was provided by the Netherlands Organization for Scientific Research NWO and by NATO grant 0148/87. Randell Stephenson and an anonymous reviewer are thanked for useful suggestions.

Appendix 1

The differential equation governing the deflection $w(x)$ of a thin elastic plate with variable rigidity $D(x)$, horizontal load N and surface load $q(x)$ on top of a fluid mantle is:

$$\frac{\mathrm{d}^2}{\mathrm{d}x^2}\left[D(x)\frac{d^2w}{\mathrm{d}x^2}\right] + N\frac{d^2w}{\mathrm{d}x^2} + (\rho_m - \rho_s)gw(x) = q(x) \quad (1)$$

with $g = 9.8$ m s^{-2} the gravity acceleration and $(\rho_m - \rho_s)$ is the density contrast of mantle and sedimentary infill.

The relationship between the flexural rigidity $D(x)$ and the thickness of the elastic plate EET (x) is:

$$D(x) = \frac{E\left[\mathrm{EET}(x)^3\right]}{12(1-\nu^2)} \quad (2)$$

in which E is Young's modulus and ν is Poisson's ratio. In this study, we adopt the following values: $E = 7.0 \times 10^{10}$ N m^{-2} and $\nu = 0.25$.

To solve the fourth-order differential eq. 1, a finite difference approximation is used.

Boundary conditions

As $x \to \infty$, $w(x) \to 0$ and $\mathrm{d}w/\mathrm{d}x \to 0$. For the extensional basin modelling, the left-hand boundary conditions are: as $x \to -\infty$, $w(x)$ *0* and $\mathrm{d}w/\mathrm{d}x \to 0$. For the foreland basin modelling, the left-hand boundary conditions for the broken plate are, at $x = 0$:

$$-D\left(\frac{\mathrm{d}^2w}{\mathrm{d}x^2}\right)\Bigg|_{x=0} = M_0 = 0 \quad (3)$$

with M_0 the bending moment applied at the free end of the plate (positive for counterclockwise).

$$\frac{\mathrm{d}}{\mathrm{d}x}D\left(\frac{\mathrm{d}^2w}{\mathrm{d}w^2}\right)\Bigg|_{x=0} = P_0 = 0 \quad (4)$$

where P_0 is the vertical shear force applied at the free end of plate (down is positive).

Appendix 2

The ongoing thermal subsidence during the foreland basin phase has been calculated by applying a vertical load F_t, which changes through time, to the broken plate model (see also Appendix 1). F_t for a certain time-step Δt calculated from the density increase of the lithosphere due to contraction during cooling:

$$F_t = \int_0^L \Delta T \rho \alpha g \, \mathrm{d}z \quad (1)$$

L denotes the lithospheric thickness in thermal equilibrium, ΔT is the temperature decrease during Δt, ρ the density of crust or mantle rocks at

surface conditions, α the coefficient of thermal expansion and g the gravity acceleration.

References

1 C. Beaumont, Foreland basins, Geophys. J.R. Astron. Soc. 65, 291–329, 1981.
2 T.E. Jordan, Thrust loads and foreland basin evolution, Cretaceous, Western United States, Am. Assoc. Pet. Geol. Bull. 65, 2506–2520, 1981.
3 G.M. Quinlan and C. Beaumont, Appalachian thrusting, lithospheric flexure and the Paleozoic stratigraphy of the eastern interior of North America, Can. J. Earth Sci. 21, 973–996, 1984.
4 G.D. Karner and A. Watts, Gravity anomalies and flexure of the lithosphere at mountain ranges, J. Geophys. Res. 88, 10449–10477, 1983.
5 L. Royden and G.D. Karner, Flexure of the lithosphere beneath the Apennine and Carpathian foredeep basins, Nature, 309, 142–144, 1984.
6 C.L. Angevine and K.M. Flanagan, Buoyant sub-surface loading of the lithosphere in the Great Plains Foreland Basin, Nature, 327, 137–139, 1987.
7 I. Moretti and L. Royden, Deflection, gravity and tectonics of doubly subdcted continental lithosphere: Adriatic and Ionian Seas, Tectonics, 7, 875–893, 1988.
8 S. Kruse and M.K. McNutt, Compensation of paleozoic orogens: a comparison of the Urals to the Appalachians, Tectonophysics, 154, 1–17, 1988.
9 H. Lyon-Caen and P. Molnar, Constraints on the structure of the Himalaya from an analysis of gravity anomalies and a flexural model of the lithosphere, J. Geophys. Res. 88, 8171–8191, 1983.
10 L. Royden, Flexural behavior of the continental lithosphere in Italy: constraints imposed by gravity and deflection data, J. Geophys. Res. 93, 7747–7766, 1988.
11 G.S. Stockmal, C. Beaumont and R. Boutilier, Geodynamic models of convergent margin tectonics: the transition from rifted margin to overthrust belt and the consequences for foreland basin development, Am. Assoc. Pet. Geol. Bull. 70, 181–190, 1986.
12 J. Chery, J.P. Vilotte and M. Daignières, Thermo-mechanical evolution of thinned continental lithosphere under compression: implications for the Pyrenees, UMSI, 89/59, Minneapolis, March 1989.
13 E. Roca and P. Desegaulx, Geodynamic evolution of the Valencia Trough from a Mesozoic extensional basin to the Early Miocene foredeep of the Betic–Balearic Chain, Mar. Pet. Geol. in press, 1989.
14 H.E. Bakker, K. de Jong, H. Helmers and C. Biermann, The geodynamic evolution of the internal zone of the Betic Cordilleras (southeast Spain): a model based on structural analysis and geothermobarometry, J. Metamorph. Geol. 7, 359–381, 1989.
15 J. Guimera, Evolution de la déformation Alpine dans le N.E. de la chaîne Iberique et dans la chaîne cotière Catalane, C.R. Acad. Sci. Paris, 297, Sér. I, 425–430, 1983.
16 P. Choukroune and ECORS Team, ECORS deep seismic data and balanced cross sections: geometric constraints on the evolution of the Pyrenees, Tectonics, 8, 23–39, 1989.
17 B. Baldwin and C.O. Butler, Compaction curves, Am. Assoc. Pet. Geol. Bull. 69, 622–626, 1985.
18 D.P. McKenzie, Some remarks on the development of sedimentary basins, Earth Planet. Sci. Lett. 40, 25–32, 1978.
19 A. Watts, G.D. Karner and M.S. Steckler, Lithospheric flexure and the evolution of sedimentary basins, Phil. Trans. R. Soc. London, Ser. A, 305, 249–281, 1982.
20 G.E. Vink, W.J. Morgan and W.L. Zhao, Preferential rifting of continents: a source of displaced terranes, J. Geophys. Res. 89, 10072–10076, 1984.
21 M.S. Steckler and U.S. Ten Brink, Lithospheric strength variations as a control on new plate boundaries: examples from the northern Red Sea region, Earth Planet. Sci. Lett. 79, 120–132, 1986.
22 M.K. McNutt, M. Diament and M.G. Kogan, Variations of elastic plate thickness at continental thrust belts, J. Geophys. Res. 93, 8825–8838, 1988.
23 S. Cloetingh, H. Kooi and W. Groenewoud, Intraplate stress and sedimentary basin evolution, Geophys. Monogr. Am. Geoph. Union, 48, 1–16, 1989.
24 N. Kuznir and G.D. Karner, Dependence of the flexural rigidity of the continental lithosphere on rheology and temperature, Nature, 316, 138–142, 1985.
25 R. Zoetemeijer, P. Desegaulx, S. Cloetingh, F. Roure and I. Moretti, Lithospheric dynamics and tectonic–stratigraphic evolution of the Ebro basin, J. Geophys. Res. 95, 2701–2711, 1989.
26 B. Pinet, Deep seismic profiling and sedimentary basins, Bull. Soc. Géol. Fr. 8, 749–766, 1989.
27 P. Choukroune and M. Mattauer, Tectonique des plaques et Pyrénées: sur le fonctionnement de la faille Nord-Pyrénéenne. Comparaison avec les modèles actuels, Bull. Soc. Géol. Fr. 20, 689–700, 1978.
28 E.J. Debroas, Modèle de bassin triangulaire à l'intersection de décrochements divergents pour le fossé albo-cénomanien de la Ballongue (Zone Nord Pyrénéenne, France), Bull. Soc. Géol. Fr. 5, 887–898, 1987.
29 R. Curnelle, Projet d'Implantation du profil "Structure profonde du Golfe de Gascogne", profil plateau Aquitaine, Internal report I.F.P. No. 33910, 16 pp., 1986.
30 P. Desegaulx and M.F. Brunet, Tectonic subsidence of the Aquitaine Basin since Cretaceous times, Bull. Soc. Géol. Fr. 295–306, 1989.
31 P. Desegaulx, F. Roure and A. Villien, Structural evolution of the Pyrenees: tectonic inheritance and flexural behaviour of the continental crust, Tectonophysics, 182, 211–225, 1990.
32 S. Kruse and L. Royden, Forces associated with post tectonic unflexing of the Adriatic lithosphere, Italy (abstr.), E.O.S. 68, No. 44, 1465, 1987.
33 L. Royden and C.E. Keen, Rifting process and thermal evolution of the continental margin of eastern Canada determined from subsidence curves, Earth Planet. Sci. Lett. 51, 343–361, 1980.
34 B. Pinet, Crustal structure of the Aquitaine shelf (Bay of Biscay) from deep seismic experiment, Nature, 235, 513–516, 1987.

Elsevier Science Publishers B.V. All rights reserved

35 G.T. Jarvis and D.P. McKenzie, Sedimentary basin formation with finite extension rates, Earth Planet. Sci. Lett. 48, 42–52, 1980.
36 J.R. Cochran, Effects of finite rifting times on the development of sedimentary basins, Earth Planet. Sci. Lett. 66, 289–302, 1983.
37 H. Kooi and S. Cloetingh, Intraplate stresses and the tectono-stratigraphic evolution of the Central North Sea, Am. Assoc. Pet. Geol. Mem. 46, 541–558, 1989.
38 G. Mathieu, Histoire géologique du sous Bassin de Parentis, Bull. Centre Rech. Explor. Prod. Elf Aquitaine, 10, 33–47, 1986.
39 M.F. Brunet, Subsidence history of the Aquitaine Basin determined from subsidence curves, Geol. Mag. London, 121, 421–428, 1984.
40 J.G. Sclater and P.A.F. Christie, Continental stretching: an explanation of the post-mid-Cretaceous subsidence of the central North Sea basin, J. Geophys. Res. 85, 3711–3739, 1980.
41 B.R.G.M., Elf-Re, Esso-Rep and S.N.P.A., Géologie du bassin d' Aquitaine, B.R.G.M. publishers, Orleans, 1974.
42 F. Marchal, Apport de la gravimétrie à la connaissance des structures profondes sous le bassin d'Aquitaine, extension de la chaîne Hercynienne, Phd thesis, Montpellier, 1986.
43 M.F. Brunet, The influence of the evolution of the Pyrenees on adjacent basins, Tectonophysics, 129, 343–354, 1986.
44 M. Séguret and M. Daignières, Crustal scale balanced cross-sections of the Pyrenees; discussion, Tectonophysics, 129, 303–318, 1986.
45 R. Wortel and S. Cloetingh, On the dynamics of convergent plate boundaries and stress in the lithosphere, in: The Origin of Arcs, F.C. Wezel, ed., pp. 115–139, Elsevier, Amsterdam, 1986.
46 J.X. Mitrovica, C. Beaumont and G.T. Jarvis, Tilting of continental interiors by the dynamical effects of subduction, Tectonics, 8, 1079–1094, 1989.
47 S. Cloetingh, Intraplate stresses: a new element in basin analysis, in: K. Kleinspehn and C. Paola, eds., New Perspectives in Basin Analysis, pp. 305–330, Springer, New York, N.Y., 1988.